Available online at www.sciencedirect.com
SCIENCE DIRECT®
Journal of Organometallic Chemistry 689 (2004) 3031–3039
Journal of Organometallic Chemistry
www.elsevier.com/locate/jorganchem

# A complete series of tricarbonylhalidorhenium(I) complexes (abpy)Re(CO)$_3$(Hal), Hal = F, Cl, Br, I; abpy = 2,2′-azobispyridine: Structures, spectroelectrochemistry and EPR of reduced forms

Stéphanie Frantz [a], Jan Fiedler [b], Ingo Hartenbach [a], Thomas Schleid [a], Wolfgang Kaim [a,*]

[a] Institut für Anorganische Chemie, Universität Stuttgart, Pfaffenwaldring 55, D-70550 Stuttgart, Germany
[b] J. Heyrovský Institute of Physical Chemistry, Academy of Sciences of the Czech Republic, Dolejškova 3, CZ-18223 Prague, Czech Republic

Received 19 March 2004; accepted 14 June 2004
Available online 6 August 2004

**Abstract**

For the first time a complete set of tricarbonylhalidorhenium(I) complexes (Hal = F, Cl, Br, I) has been studied in a systematical fashion by example of (abpy)Re(CO)$_3$(Hal), abpy = 2,2′-azobispyridine. Crystal structures of chloride, bromide and iodide analogues are now available, showing increasing planarization of the abpy ligand in that order. Cyclic voltammetry, EPR, IR and UV/Vis spectroelectrochemistry of the reduced forms [(abpy)Re(CO)$_3$(Hal)]$^{\cdot-}$ illustrate that the four halide complexes differ only partially in their properties. The strongest deviations are observed for [(abpy)Re(CO)$_3$F]$^{\cdot-}$ which is distinguished by the widest electrochemical potential range but most pronounced chemical lability. In the EPR spectrum the fluoride exhibits the highest isotropic $g$ value (2.0085) and the lowest rhenium coupling constant, which is of the same magnitude (2 mT) as the detectable $^{19}$F hyperfine splitting.


*Keywords:* Crystal structures; Electrochemistry; EPR spectroscopy; Halide variation; Rhenium complexes

## 1. Introduction

Since the discovery that (bpy)Re(CO)$_3$Cl can act as an efficient electrocatalyst for the reduction of $CO_2$ [1,2] many complexes of the type (N^N)Re(CO)$_3$(Hal) with N^N = α-diimine or related chelate ligand have been the subject of studies in the context of photo- or electrocatalyzed $CO_2$ reduction [3–5]. The primary activation mechanism involves the addition of an electron to the π* orbital of the N^N ligand with the result of a labilization of the halide as essential step [5–7].

Although complexes (N^N)Re(CO)$_3$(Hal) have thus been well studied, a complete set with Hal = F, Cl, Br, I, is known only for N^N = bpy = 2,2′-bipyridine [3,6–8]. Even there the fluoride and iodide complexes were not extensively characterized [7,8]. In any case, very few complexes are known containing the Re(CO)$_3$F fragment [8]. In summary, no systematic study of the influence of the halide on such a system has been carried out yet. In this work, we describe the complete series (abpy)Re(CO)$_3$(Hal), Hal = F, Cl, Br, I; abpy = 2,2′-azobispyridine [9] (see Fig. 1).

* Corresponding author. Tel.: +49-711-685-4170/4171; fax: +49-711-685-4165.
*E-mail address:* kaim@iac.uni-stuttgart.de (W. Kaim).

0022-328X/$ - see front matter © 2004 Elsevier B.V. All rights reserved.
doi:10.1016/j.jorganchem.2004.06.047

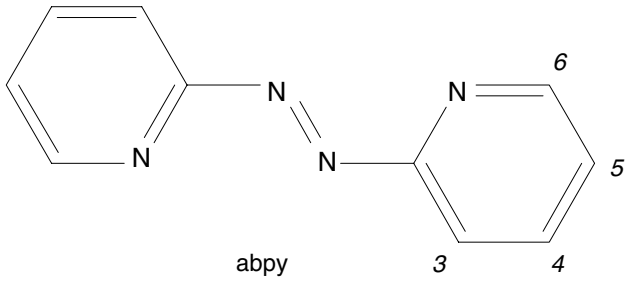


Fig. 1. The ligand abpy.

The complexes (abpy)Re(CO)$_3$(Hal) with Hal = Cl and Br [6c,7] were reported earlier. The chloride derivative has been characterized structurally [6c]. The bromide and iodide were described recently [10] as precursors for heterodinuclear complexes of the potentially bridging [9] abpy. The chloride and bromide complexes undergo a two-step reduction [6c,7]. The first step consists of a reversible ligand-centered electron transfer. The second step is an EC process, leading to the loss of the halide which is accompanied by substitution with solvent molecules and can lead to dimerization [7]. In this report the fluoride and iodide analogues as well as additional studies of (abpy)Re(CO)$_3$Br will be reported. Results from NMR spectroscopy, structural characterization (Br, I species), electrochemistry, UV/Vis, IR and EPR spectroscopy of reduced forms will be discussed.

## 2. Results and discussion

### 2.1. Syntheses and characterization

The complexes (abpy)Re(CO)$_3$(Hal) (Hal = F, Br, I) were synthesized by the same route as (abpy)Re(CO)$_3$Cl [6c] (Fig. 2) with increasing reaction times while going from F to I.

The precursors Re(CO)$_5$(Hal) for the preparation of the bromide and iodide complexes were either commercially available (bromide) or easy to synthesize (iodide [11]). The precursor Re(CO)$_5$F has been reported earlier [8]. However, it is difficult to isolate and oligomerizes to [Re(CO)$_3$F]$_4$ under heating. Its synthesis was therefore adapted from the known procedure [8], and the addition of the abpy ligand was carried out in situ according to the following scheme:

$$\mathrm{Re(CO)_5I} + 6\mathrm{AgF} \xrightarrow[\mathrm{RT,2\,h}]{\text{toluene}} \mathrm{Re(CO)_5F} \xrightarrow[40\,^{\circ}\mathrm{C,1\,h}]{+\text{abpy}/-2\mathrm{CO}} (\text{abpy})\mathrm{Re(CO)_3F} \quad (1)$$

The $^1$H NMR spectra show the expected pattern [6c,9]. The signals are shifted to lower field with respect to the signals of the free ligand (Table 1). Variation of the halogen atoms has little influence on the $^1$H NMR chemical shifts, the results point to a similar configuration for all complexes.

### 2.2. Crystal structures

The crystal structure of (abpy)Re(CO)$_3$Cl has been reported earlier [6c]. Single crystals of the complexes (abpy)Re(CO)$_3$Br and (abpy)Re(CO)$_3$I could be obtained by slow evaporation of $CH_2Cl_2$ solutions layered with hexane. Crystallographic data are given in Table 2 and in the Section 3. Selected bond lengths and bond angles are listed in Tables 3 and 4. The molecular structure of the iodide compound is shown in Fig. 3. It was not possible to crystallize the fluoride complex which decomposes on prolonged storage in solution.

Only subtle changes are observed in the molecular structures on going from the chloride to the iodide complex. All three structures confirm the facial arrangement of the three carbonyl groups at rhenium(I). The abpy ligand adopts an *s-cis*/*E*/*s-trans* conformation as already observed for the related (abpy)Mo(CO)$_4$ [12].

The bond lengths in the newly crystallized complexes are in good agreement with those of previously reported [6c,12] structures (Table 3). The azo bond lengths (N1–N3) are at ≈1.28 Å for all derivatives, confirming a similar amount of π back donation from the rhenium(I) center into the π*(abpy) orbital by comparison with the value of the free ligand (1.246(2) Å [9]). The rhenium bond lengths to the better σ donating but weaker π accepting pyridyl nitrogen (N2) and the better π accepting but less basic azo nitrogen (N1) atoms are of a similar magnitude for all analogues. As expected, the Re–Hal bond distance increases from 2.475(4) Å for the chloride to 2.8045(11) Å for the iodide analogue via 2.607(2) Å for the bromide. Accordingly, the Re–C1 and the C1–O1 bonds *trans* to the halide should be most affected by the change of halogen. For the iodide a lengthening of the Re–C1 bond is observed (2.04(2) Å vs. 1.916(14)

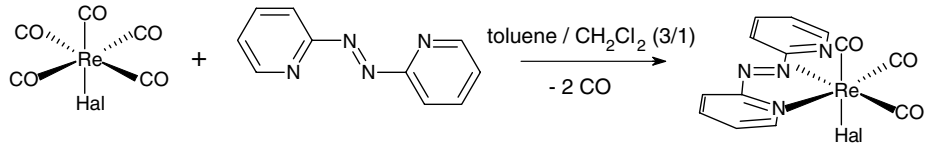


Fig. 2. Synthesis of (abpy)Re(CO)$_3$(Hal) (Hal = F, Br, I).

Table 1
$^1$H NMR data[a] of the complexes (abpy)Re(CO)$_3$(Hal) and of free abpy at 250 MHz

| | $\delta$/ppm | | | |
|---|---|---|---|---|
| | $H^{6,6'}$ | $H^{5,5'}$ | $H^{4,4'}$ | $H^{3,3'}$ |
| abpy[b] | 8.76 | 7.48 | 7.94 | 7.86 |
| (abpy)Re(CO)$_3$F[b] | 9.12/8.82 | 7.68/7.61 | 8.24/7.94 | 8.66/8.12 |
| (abpy)Re(CO)$_3$Cl[c] | 9.12/8.83 | 7.72/7.66 | 8.29/8.05 | 8.71/8.15 |
| (abpy)Re(CO)$_3$Br[b] | 9.15/8.80 | 7.65/7.60 | 8.21/7.94 | 8.68/8.11 |
| (abpy)Re(CO)$_3$I[b] | 9.22/8.78 | 7.60/7.57 | 8.18/7.94 | 8.72/8.11 |

[a] $H^{n'}$ indicates a proton in the uncoordinated part of the ligand. The coupling constants are standard for 2-pyridyl substituents.
[b] In $CDCl_3$.
[c] In $CD_2Cl_2$.

Table 2
Crystallographic data and refinement parameters

| | (abpy)Re(CO)$_3$Br | (abpy)Re(CO)$_3$I |
|---|---|---|
| Empirical formula | $C_{13}H_8BrN_4O_3Re$ | $C_{13}H_8IN_4O_3Re$ |
| Formula weight (g mol$^{-1}$) | 534.34 | 581.33 |
| Crystal size (mm) | $0.4 \times 0.4 \times 0.2$ | $0.4 \times 0.1 \times 0.1$ |
| Crystal system | Monoclinic | Monoclinic |
| Space group | *Cc* | $P2_1/c$ |
| Unit cell dimensions | | |
| $a$ (Å) | 13.6481(4) | 14.0765(7) |
| $b$ (Å) | 9.0644(2) | 9.1370(5) |
| $c$ (Å) | 12.3607(3) | 12.3395(6) |
| $\beta$ (°) | 98.663(1) | 97.521(2) |
| Cell volume (Å$^3$) | 1511.72(7) | 1573.42(14) |
| Calculated density (g cm$^{-3}$) | 2.348 | 2.454 |
| Absorption coefficient (mm$^{-1}$) | 10.70 | 9.70 |
| $2\theta_{max}$ (°) | 55.00 | 55.03 |
| Index ranges | $-17 \leqslant h \leqslant 17$; $-11 \leqslant k \leqslant 11$; $-15 \leqslant l \leqslant 16$ | $-18 \leqslant h \leqslant 18$; $-11 \leqslant k \leqslant 11$; $-16 \leqslant l \leqslant 15$ |
| Formula units per cell ($Z$) | 4 | 4 |
| Reflections collected | 18,133 | 26,223 |
| Unique reflections | 3464 | 3598 |
| $R_{int}/R_\sigma$ | 0.0708/0.0395 | 0.0651/0.0286 |
| Goodness-of-fit, GOF ($F^2$) | 1.143 | 1.185 |
| Data/restraints/parameters | 3464/2/200 | 3598/0/200 |
| Flack-X parameter | −0.02(3) | |
| $R$ indices (for all data) | $R_1 = 0.0627$; $wR_2 = 0.1646$ | $R_1 = 0.0683$; $wR_2 = 0.1574$ |
| Extinction | 0.0027(4) | 0.0014(2) |
| Largest residual electron densities (e Å$^{-3}$) | 5.90, −2.23 | 2.35, −1.95 |

GOF $= \{\sum_w(|F_o|^2 - |F_c|^2)^2/(n-m)\}^{1/2}$ where $n$ = number of data and $m$ = number of variables; $R = (\sum ||F_o| - |F_c||)/\sum |F_o|$; $wR = \{\sum[w(|F_o|^2 - |F_c|^2)^2]/\sum[w(F_o^4)]\}^{1/2}$.

and 1.888(15) Å for the chloride and bromide derivatives, respectively), coupled with a shortening of the C1–O1 bond. The extremely short C1–O1 bond of 0.92(2) Å for the iodide is a consequence of intermolecular interactions: The packing of the (abpy)Re(CO)$_3$(Hal) molecules with their largely planar (abpy)Re(CO$_{eq}$)$_2$ units in the crystal differs. Whereas the molecules with Hal = Br or Cl are packed with the Re–Hal bonds oriented in only one direction, the iodide complex molecules show an alternating behavior, leading to non-bonded neighboring iodide atoms with $d$(I···I) = 5.080 Å. This different packing of (abpy)Re(CO)$_3$I causes contacts of about 3.4–3.5 Å between O1 and C or N atoms of neighboring molecules. As a result, the vibrational ellipsoid for O1 adopts a different shape (Fig. 3), the C1–O1 distance appears unusually short (Table 3), and the angle Re–C1–O1 decreases.

Fig. 3 and Table 4 illustrate that the alignment halide/rhenium/*trans*-CO becomes generally somewhat less linear with the increasing size of the halide. Furthermore, the dihedral angle $\omega$ between the planes of the uncoordinated pyridine ring and the rest of the coordinated abpy becomes distinctly smaller when going from the chloride (16.1°) to the iodide (4.0°) compound, illustrating a tendency of the ligand to become completely planar.

Table 3
Selected bond lengths (Å) for (abpy)Re(CO)$_3$(Hal)

| | abpy[a] | Hal = Cl[b] | Hal = Br[c] | Hal = I[c] |
|---|---|---|---|---|
| N1–N3 | 1.246(2) | 1.272(9) | 1.274(16) | 1.288(15) |
| N1–Re | – | 2.143(5) | 2.145(10) | 2.125(10) |
| N2–Re | – | 2.145(6) | 2.154(10) | 2.143(10) |
| Re–Hal | – | 2.475(4) | 2.607(2) | 2.8045(11) |
| Re–C1 | – | 1.916(14) | 1.888(15) | 2.04(2) |
| Re–C2 | – | 1.918(8) | 1.931(17) | 1.895(17) |
| Re–C3 | – | 1.941(8) | 1.944(14) | 1.937(14) |
| C1–O1 | – | 1.156(16) | 1.17(2) | 0.92(2) |
| C2–O2 | – | 1.152(12) | 1.14(3) | 1.167(19) |
| C3–O3 | – | 1.133(10) | 1.130(18) | 1.144(16) |

[a] Refs. [9,13].
[b] Data collection at 173 K [6c].
[c] Data collection at 293 K.

Table 4
Selected angles (°) for (abpy)Re(CO)$_3$(Hal)

| | Hal = Cl[b] | Hal = Br[c] | Hal = I[c] |
|---|---|---|---|
| $\omega$[a] | 16.1 | 13.4 | 4.0 |
| C1–Re–C2 | 90.0(4) | 89.3(7) | 89.6(7) |
| C1–Re–C3 | 86.5(9) | 86.7(6) | 87.3(6) |
| O1–C1–Re | 177.9(9) | 178.5(14) | 172.5(17) |
| O2–C2–Re | 176.4(9) | 178.2(18) | 176.8(15) |
| O3–C3–Re | 178.4(8) | 177.5(15) | 177.2(13) |
| C1–Re–Hal | 177.0(3) | 176.1(4) | 175.2(4) |
| C2–Re–Hal | 91.7(3) | 91.3(6) | 89.9(5) |
| C3–Re–Hal | 91.1(3) | 89.4(5) | 87.9(4) |
| N1–Re–Hal | 85.3(2) | 85.5(3) | 87.9(3) |
| N2–Re–Hal | 84.9(2) | 85.9(3) | 86.3(3) |
| C1–Re–N1 | 93.5(3) | 94.7(5) | 93.3(5) |
| C1–Re–N2 | 97.3(3) | 97.8(5) | 98.4(5) |

[a] Dihedral angle between the planes of the uncoordinated pyridine ring and the rest of coordinated abpy.
[b] Data collection at 173 K [6c].
[c] Data collection at 293 K.

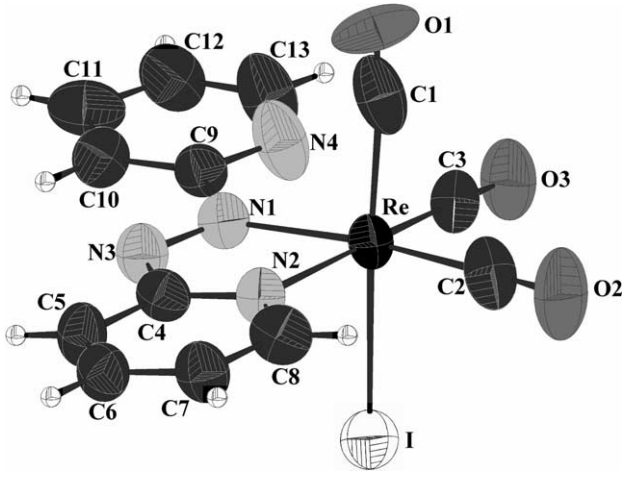


Fig. 3. Molecular structure of (abpy)Re(CO)$_3$I in the crystal.

## 2.3. Cyclic voltammetry

The complexes (abpy)Re(CO)$_3$(Hal) with Hal = F and I undergo electrochemical processes analogous to those of the chloride [6c] and bromide [7] species (Fig. 4). They display a reversible first reduction, assigned to adding one electron to the $\pi^*$ orbital of the abpy ligand. The second reduction occurs in an irreversible step with release of the halide ligand, the follow-up product [(abpy)Re(CO)$_3$]$^-$ can be re-oxidized at a more positive potential [6c,7]. The data for the four analogues are summarized in Table 5.

When going from the fluoride to the iodide complex the first reduction potentials display relatively little variation. However, the fluoride complex is easiest to reduce, reflecting the high electronegativity of F. For the second (halide-dissociative) reduction, the peak potentials $E_{2pc}$ become less negative with increasing Re–Hal bond lengths (Table 5). As a result, the fluoride complex thus shows the largest value $|E_{2pc} - E_1|$ at 0.84 V, i.e., the widest potential range and thus the highest comproportionation constant for the radical state [(abpy)Re(CO)$_3$Hal)]$^{\bullet-}$.

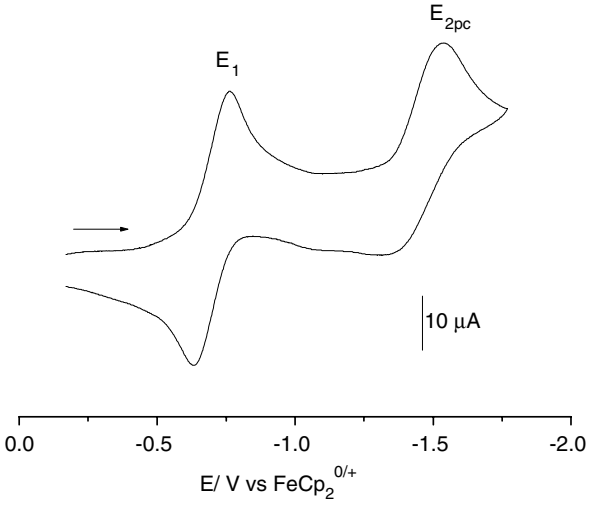


Fig. 4. Cyclic voltammogram of (abpy)Re(CO)$_3$F in $CH_2Cl_2$/0.1 M $Bu_4NPF_6$.

Table 5
Electrochemical potentials[a] from cyclic voltammetry[b]

| | $E_1$[c] | $E_{2pc}$[d] | $\lvert E_{2pc} - E_1 \rvert$ |
|---|---|---|---|
| (abpy)Re(CO)$_3$F[e] | −0.70 | −1.54 | 0.84 |
| (abpy)Re(CO)$_3$Cl[e,f] | −0.78 | −1.54 | 0.76 |
| (abpy)Re(CO)$_3$Br[e] | −0.78 | −1.42 | 0.66 |
| (abpy)Re(CO)$_3$Br[g] | −0.80 | −1.49 | 0.69 |
| (abpy)Re(CO)$_3$I[e] | −0.79 | −1.33 | 0.54 |

[a] In V vs. $FeCp_2^{0/+}$.
[b] At 100 mV/s scan rate.
[c] Half-wave potential corresponding to a reversible step.
[d] Cathodic peak potential corresponding to an irreversible step.
[e] In $CH_2Cl_2$/0.1 M $Bu_4NPF_6$ at a glassy carbon electrode at 298 K.
[f] Ref. [6c].
[g] In THF/0.1 M $Bu_4NPF_6$ at a platinum disk electrode at 298 K [7].

### 2.4. IR spectroelectrochemistry

IR spectroelectrochemical investigations were carried out in $CH_2Cl_2$/0.1 M $Bu_4NPF_6$ solutions in an Optically Transparent Thin Layer Electrochemical (OTTLE) cell [14]. The measurements were performed to study the reduction mechanism of the complexes. Through this method the changes of the electronic structure can be examined. The emergence of isosbestic points for the different reduction steps confirms the homogeneity of the experiments (Figs. 5 and 6).

IR spectroelectrochemistry was performed in the carbonyl stretching region which allows to examine changes of symmetry in the molecule.

The results of the experiments for the new and for the previously investigated complexes (abpy)Re(CO)$_3$(Hal) are summarized in Table 6.

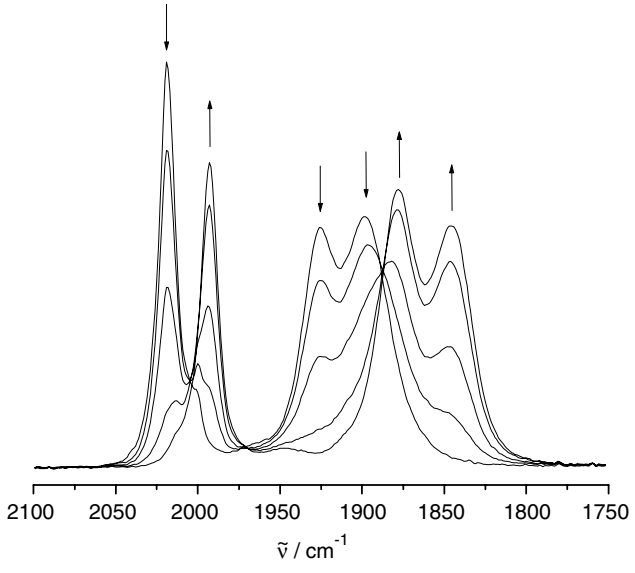


Fig. 5. IR Spectroelectrochemical reduction at $E_1$ of (abpy)-Re(CO)$_3$F → [(abpy)Re(CO)$_3$F]$^{\cdot-}$ in $CH_2Cl_2$/0.1 M $Bu_4NPF_6$.

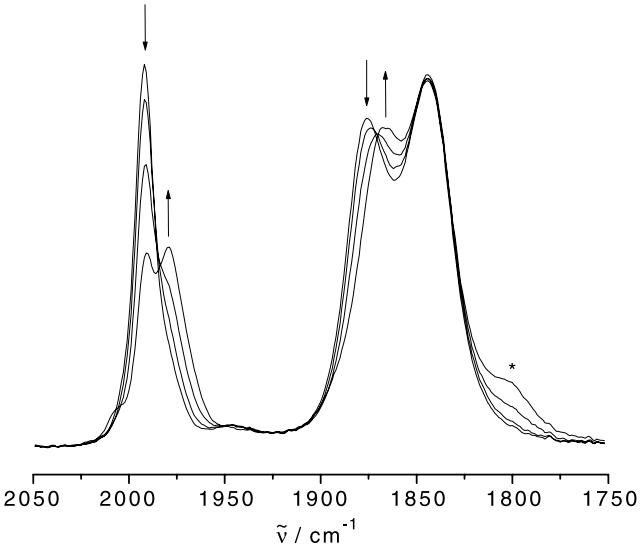


Fig. 6. IR Spectroelectrochemical reduction at $E_{2pc}$ of [(abpy)-Re(CO)$_3$F]$^{\cdot-}$ → [(abpy)Re(CO)$_3$]$^-$ in $CH_2Cl_2$/0.1 M $Bu_4NPF_6$ (the band marked with * is assigned to a decomposition product).

The newly synthesized fluoride and iodide complexes show a similar behavior as the chloride [6c] and bromide [7] analogues. The compounds exhibit the expected three separated bands for non-symmetrically substituted *fac*-(CO)$_3$Re moieties with one sharp band ($A_1$) at high frequency and two bands (split E) at lower energies (Fig. 5). The bands are at lower values by about 20 cm$^{-1}$ for (abpy)Re(CO)$_3$F, in agreement with the high electronegativity of F.

Upon one-electron reduction, the expected [6c,7] shift of all bands to lower energies is observed (Fig. 5). Through uptake of an electron the π back bonding between metal and abpy is reduced which in turn enhances M–CO π back-donation and weakening of the C–O bond. The same trend is observed for both (abpy)Re(CO)$_3$(Hal) and (bpy)Re(CO)$_3$(Hal) complexes [6,7]. However, the shifts are more pronounced for the complexes of the better π accepting ligand abpy.

After uptake of another electron the complexes exhibit a four-band pattern, suggesting a chemical change. The shifts between the one-electron and the two-electron reduced species are smaller than the shifts between the initial states and the one-electron reduced forms. This points to a conservation of charge between the first and the second reduction. The similarity of band positions after the irreversible second reduction of the fluoride and iodide complexes points to formation of the same compound. Loss of the halide was postulated earlier for the chloride and bromide analogues [6c,7], in analogy to results for (bpy)Re(CO)$_3$(Hal).

The proposed mechanism for the reduction of (abpy)Re(CO)$_3$(Hal) is summarized in (2).

Table 6
IR vibrational data from spectroelectrochemistry of (abpy)Re(CO)$_3$(Hal) in 0.1 M *n*-Bu$_4$NPF$_6$ solutions

| Complex | Solvent | $\tilde{\nu}_{CO}$ (cm$^{-1}$) | | |
|---|---|---|---|---|
| (abpy)Re(CO)$_3$F | $CH_2Cl_2$ | 2018(vs) | 1925(s) | 1898(s) |
| [(abpy)Re(CO)$_3$F]$^{\bullet-}$ | $CH_2Cl_2$ | 1993(vs) | 1878(s) | 1846(s) |
| [(abpy)Re(CO)$_3$]$^-$[a] | $CH_2Cl_2$ | 1991(s)/1979(s) | 1867(s) | 1844(s) |
| (abpy)Re(CO)$_3$Cl [6c] | DCE[b] | 2030(vs) | 1943(s) | 1917(s) |
| [(abpy)Re(CO)$_3$Cl]$^{\bullet-}$ [6c] | DCE[b] | 2004(vs) | 1898(s) | 1866(s) |
| (abpy)Re(CO)$_3$Br | $CH_2Cl_2$ | 2032(vs) | 1947(s) | 1922(s) |
| (abpy)Re(CO)$_3$Br [7] | THF | 2028(s) | 1943(s) | 1917(s) |
| [(abpy)Re(CO)$_3$Br]$^{\bullet-}$ [7] | THF | 2004(s) | 1900(s) | 1871(s) |
| (abpy)Re(CO)$_3$I | $CH_2Cl_2$ | 2029(vs) | 1941(s) | 1921(s) |
| [(abpy)Re(CO)$_3$I]$^{\bullet-}$ | $CH_2Cl_2$ | 2001(vs) | 1893(s) | 1861(s) |
| [(abpy)Re(CO)$_3$]$^-$[c] | $CH_2Cl_2$ | 1989(s)/1980(s) | 1869(s) | 1842(s) |

[a] From two-electron reduction of fluoride complex.
[b] DCE = 1,2-dichloroethane.
[c] From two-electron reduction of iodide complex.

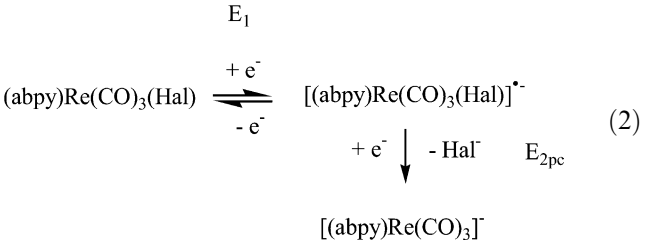


(2)

### 2.5. UV/Vis spectroelectrochemistry

The results from the experiments with the (abpy)Re(CO)$_3$(Hal) complexes are listed in Table 7.

The neutral complexes (abpy)Re(CO)$_3$(Hal) exhibit metal(Re)-to-ligand(abpy) charge transfer (MLCT) bands between 565 and 592 nm. Another band at about 350 nm is tentatively assigned to an intra-ligand transition.

On one-electron reduction the complexes [(abpy)Re(CO)$_3$(Hal)]$^{\bullet-}$ exhibit the typical narrow intra-ligand bands of azoaromatic radical anions at about 400 nm (Table 7) with rather high intensity. The MLCT bands are shifted to about 500 nm due to the diminished π-acceptor ability of the abpy$^{\bullet-}$ ligand compared to neutral abpy.

Upon the second, irreversible reduction the MLCT bands vanish and a band at 440 nm appears (Table 7 [7]).

### 2.6. EPR spectroscopy

The one-electron reduced species are radical complexes ($S = 1/2$) where an anion radical ligand is bound to a diamagnetic transition metal fragment. In such cases EPR gives three sources of information [16]:

*The isotropic g value*, with deviations from the free electron value of 2.0023 attributed to the contribution of excited states with non-zero angular momentum to the radical ground state. Thus, the spin–orbit interaction becomes essential, and the spin–orbit coupling constant

Table 7
Absorption data obtained from UV/Vis spectroelectrochemistry of (abpy)Re(CO)$_3$(Hal) in 0.1 M *n*-Bu$_4$NPF$_6$ solutions

| Compound | Solvent | $\lambda_{max}$/nm ($\varepsilon$/10$^3$ M$^{-1}$ cm$^{-1}$) |
|---|---|---|
| abpy [15] | DMF | 312(8.7), 470(0.9) |
| abpy$^{\bullet-}$ [15] | DMF | 286sh, 360sh, 408(26.5), 548(2.6) |
| abpy$^{2-}$ [15] | DMF | 275sh, 342sh, 358(14.2), 380sh,450sh |
| (abpy)Re(CO)$_3$F | $CH_2Cl_2$ | 235sh, 290sh, 350(16.3), 570(6.0) |
| [(abpy)Re(CO)$_3$F]$^{\bullet-}$ | $CH_2Cl_2$ | 290sh, 382(15.9), 496(5.4), 580sh |
| [(abpy)Re(CO)$_3$]$^-$[a] | $CH_2Cl_2$ | 250(20.0), 376(9.2), 440(7.3) |
| (abpy)Re(CO)$_3$Cl [6c] | DCE | 320(5.8), 360(6.7), 565(2.7) |
| [(abpy)Re(CO)$_3$Cl]$^{\bullet-}$ [6c] | DCE | 392(10.1), 502(2.2) |
| [(abpy)Re(CO)$_3$]$^-$ [6c][b] | DCE | 295(8.0), 320(6.3), 440(3.2) |
| (abpy)Re(CO)$_3$Br | $CH_2Cl_2$ | 260sh, 345(6.4), 570(2.4) |
| (abpy)Re(CO)$_3$Br [7] | THF | 345, 570 |
| [(abpy)Re(CO)$_3$Br]$^{\bullet-}$ [7] | THF | 380, 500 |
| (abpy)Re(CO)$_3$I | $CH_2Cl_2$ | 230sh, 260sh, 352(9.4), 592(2.3) |
| [(abpy)Re(CO)$_3$I]$^{\bullet-}$ | $CH_2Cl_2$ | 240sh, 285sh, 340sh, 383(9.9), 496(3.0), 560sh |
| [(abpy)Re(CO)$_3$]$^-$[c] | $CH_2Cl_2$ | 242(21.0), 291(8.9), 320(7.6), 440(4.0) |

[a] From two-electron reduction of fluoride complex.
[b] From two-electron reduction of chloride complex.
[c] From two-electron reduction of iodide complex.

increases considerably with the atomic number. Paramagnetic species involving rhenium or the heavier halogens should therefore exhibit strong effects if these atoms are significantly involved in the spin distribution.

*The g anisotropy ($g_1$–$g_3$)* from measurements of powders or glassy frozen solutions is also dependent on contributions from elements with high spin–orbit coupling constants.

*The hyperfine coupling* between the unpaired electron and the various nuclei of the radical species is a most informative source of insight from EPR. However, the intrinsic line-width may be too large for the resolution of the complete hyperfine structure, the dominant metal hyperfine splitting can obscure the hyperfine splitting from the spin-bearing ligand atoms, and the low natural abundance and/or low nuclear magnetic moment of isotopes can lead to undetectable hyperfine coupling.

The electrochemically generated species [(abpy)$Re(CO)_3(Hal)]^{\cdot -}$ show a dominant splitting arising from the interaction of one rhenium center with one unpaired electron (Fig. 7). Rhenium has two naturally occuring istopes: $^{185}$Re (37.4% abundance; $I = 5/2$; $a_0 = 1253.60$ mT) and $^{187}$Re (62.6%; $I = 5/2$; $a_0 = 1266$ mT). These are the largest isotropic hyperfine coupling constants $a_0$ of all transition metal elements [17,18], and since the total abundance is 100%, the coupling is clearly visible. The fluoride complex shows a more complicated hyperfine pattern than the other three analogues. This is attributed to the interaction of the electron spin with both the rhenium *and* the fluorine ($I = 1/2$ for $^{19}$F, 100%) isotopes. Coupling from other nuclei ($^1$H, $^{14}$N, other halogen atoms) is not resolved due to broad lines and less favorable properties of the other halogen nuclei (Table 8). The presence of heavy atoms having sizeable nuclear quadrupole moments favors EPR line broadening [17].

In agreement with previous reports [6] simple first-order EPR hyperfine simulations as shown in Fig. 7 do not perfectly reproduce the experimental spectra of rhenium-containing radicals. Additional signals may also arise after prolonged electrolysis which can be attributed to partial decomposition.

The isotropic $g$ values (Table 8) are rather close to the values of the free electron (2.0023) and to the value of $abpy^{\cdot -}$ (2.0044 [9]) which confirms that the first reduction is a ligand-centered process. The highest $g_{iso}$ value and thus largest deviation was determined for the fluoride complex despite the smallest spin–orbit coupling constant of the F atom in the halogen series. The $g$ values suggest the same orbital configuration for all complexes. In frozen solutions at X-band frequency nearly isotropic signals were detected. The chemical sensitivity of these paramagnetic complexes precluded EPR measurements at very high frequencies which usually require ex situ radical generation [18].

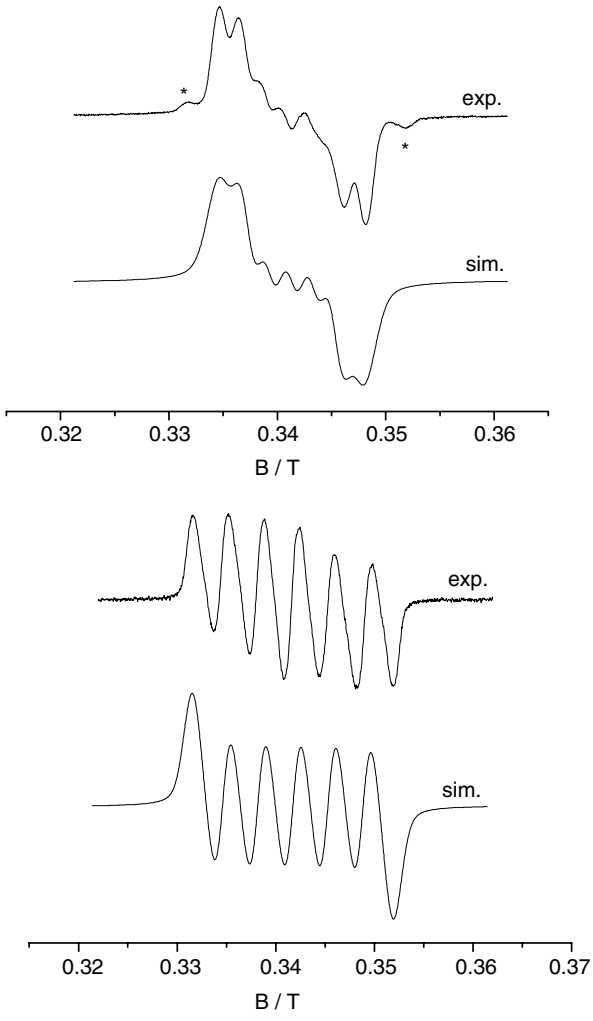


Fig. 7. Experimental and simulated EPR spectra of [(abpy)-$Re(CO)_3(Hal)]^{\cdot -}$ with Hal = F (top, linewidth 2.1 mT, ∗ signals arising after prolonged electrolysis) and Br (bottom).

The isotropic rhenium hyperfine coupling constants increase with the size of the halogen ligand, the values for the bromide and iodide complexes are comparable. This can be explained by the Re–Hal bond length increase while going from F to I, so that the spin is less delocalized for the heavier homologues (decrease of the Fermi contact interaction). Accordingly, the enhancement of the halide hyperfine coupling is noteworthy. Fluorine has the largest isotropic hyperfine coupling constant $a_0$ in the halogen series [17] which contributes to the rather large coupling constant of 1.95 mT.

Summarizing, this first systematic study of a complete halide series $[(N\hat{}N)Re(CO)_3(Hal)]^{0/\cdot -}$ showed many similarities in structures and spectroscopic properties. However, techniques very sensitive to the electronic structure such as EPR show distinct differences, reflecting subtle electronic effects such as atomic orbital overlap or spin–orbit coupling. As may have been

Table 8
EPR data for complexes $[(abpy)Re(CO)_3(Hal)]^{\cdot -}$ [a]

| X | Halogen isotopes | Natural abundance (%) | $I$ | $a_0$ [b] (mT) | $\zeta$ [c] ($cm^{-1}$) | $a_{Re}$ [d] (mT) | $a_X$ [e] (mT) | $g_{iso}$ [f] |
|---|---|---|---|---|---|---|---|---|
| F | $^{19}F$ | 100 | 1/2 | 1886.53 | 271 | 2.00 | 1.95 | 2.0085 |
| Cl | $^{35}Cl$ | 75.77 | 3/2 | 204.21 | 440 | 2.38 | n.r. | 2.0041 |
| | $^{37}Cl$ | 24.23 | 3/2 | 169.98 | | | | |
| Br | $^{79}Br$ | 50.69 | 3/2 | 1144.34 | 1842 | 3.55 | <0.65 | 2.0060 |
| | $^{81}Br$ | 49.31 | 3/2 | 1233.52 | | | | |
| I | $^{127}I$ | 100 | 5/2 | 1484.40 | n.a. | 3.50 | <0.30 | 2.0055 |

[a] Experimental values obtained after electrolysis in 0.1 M $Bu_4NPF_6/CH_2Cl_2$ solutions at 298 K.
[b] $a_0$: Isotropic hyperfine coupling constant of halogen [17].
[c] $\zeta$: Spin–orbit coupling constant of halogen [19].
[d] $a_{Re}$: $^{185/187}Re$ hyperfine coupling constant obtained from simulation.
[e] $a_X$: Halogen hyperfine coupling constant obtained from simulation.
[f] $g_{iso}$: Isotropic $g$ value.

anticipated, the effects of halide variation are small but most pronounced for the chemically least easily accessible fluoride derivative. The well known photophysical activity of such rhenium(I) compounds [20] may also show differences between analogous members of a halide series; corresponding studies are planned for the future.

## 3. Experimental

### 3.1. Instrumentation

EPR spectra were recorded in the X band on a Bruker System ESP 300 equipped with a Bruker ER035M gaussmeter and a HP 5350B microwave counter. $^1H$ NMR spectra were taken on a Bruker AC 250 spectrometer, infrared spectra were obtained using Philips PU 9800 and Perkin–Elmer 1760X FTIR instruments. UV/Vis absorption spectra were recorded on Bruins Instruments Omega 10 and HP 8453 spectrophotometers. Cyclic voltammetry was carried out at 100 mV/s scan rate in dichloromethane/0.1 M $Bu_4NPF_6$ using a three-electrode configuration (glassy carbon working electrode, Pt counter electrode, Ag/AgCl reference) and a PAR 273 potentiostat and function generator. The ferrocene/ferrocenium couple served as internal reference. Spectroelectrochemical measurements were performed using an optically transparent thin-layer electrode (OTTLE) cell [14] for UV/Vis/IR spectra and a two-electrode capillary for EPR studies [21].

### 3.2. Syntheses

#### 3.2.1. $(abpy)Re(CO)_3F$

A mixture of 175 mg (0.38 mmol) $Re(CO)_5I$ [11] and 450 mg (3.57 mmol) AgF in 30 ml toluene was stirred in the dark for 2 h. The precipitated AgI and the remaining AgF were filtered off several times. A solution of 63 mg (0.34 mmol) abpy in 5 ml toluene was added to the pale yellow filtrate and a violet color was observed immediately. The mixture was allowed to stir for 1 h at 50 °C. The violet solution was then evaporated to half the volume and 25 ml hexane were added. The solution was kept at −25 °C overnight to form a precipitate which was collected and dried under vacuum. Yield: 130 mg (0.28 mmol, 75%). Calc. for $C_{13}H_8FN_4O_3Re$ (473.43 g/mol): C, 32.98; H, 1.70; N, 11.83. Found: C, 33.68; H, 1.82; N, 11.62%.

The synthesis of Cl, Br and I analogues has been reported previously [6c,10].

### 3.3. Crystallography

Deep violet plates of $(abpy)Re(CO)_3Br$ and green needles of $(abpy)Re(CO)_3I$ for X-ray diffraction were obtained by slow evaporation of solutions in dichloromethane layered with hexane.

Data were collected on a four-circle diffractometer NONIUS Kappa-CCD with a Mo-K$\alpha$ radiation of 0.71073 Å (graphite-monochromatized) at 293 K. The crystals were sealed in capillaries for the measurements.

The structures were solved via direct methods using the programme SHELXS-97 [22]. Refinement was carried out by the full matrix least-squares method employing the programme SHELXL-97 [23]. All non-hydrogen atoms were refined anisotropically, hydrogen atoms were introduced at appropriate positions with coupled isotropic factors using the riding model. Absorption corrections were performed numerically using the programme HABITUS [24]. The programme DIAMOND 2.1e [25] was used for structure drawing.

## 4. Supplementary material

Crystallographic data have been deposited with the Cambridge Crystallographic Data Centre, CCDC-233767 and CCDC-233768. Copies of the information may be obtained free of charge from: The Director, CCDC, 12 Union Road, Cambridge CB2 1EZ, UK

(fax: (+44)1223-336-033; e-mail: deposit@ccdc.cam.ac.uk; www: http://www.ccdc.cam.ac.uk).

## Acknowledgements

This work has been supported by the Deutsche Forschungsgemeinschaft (Graduiertenkolleg "Magnetische Resonanz"), by the Fonds der Chemischen Industrie and by the European Union (COST action D14).

## References

[1] J. Hawecker, J.M. Lehn, R. Ziessel, J. Chem. Soc., Chem. Commun. (1984) 328.
[2] B.P. Sullivan, T.J. Meyer, J. Chem. Soc., Chem. Commun. (1984) 1244.
[3] (a) J. Hawecker, J.M. Lehn, R. Ziessel, Helv. Chim. Acta 69 (1986) 1900;
(b) B.P. Sullivan, C.M. Bolinger, T.D. Conrad, W. Vining, T.J. Meyer, J. Chem. Soc., Chem. Commun. (1985) 1414;
(c) T.R. O'Toole, L.D. Margerum, T.D. Westmoreland, W. Vining, R.W. Murray, T.J. Meyer, J. Chem. Soc., Chem. Commun. (1985) 1416;
(d) C.R. Cabrerea, H.D. Abruna, J. Electroanal. Chem. 209 (1986) 101;
(e) F.P.A. Johnson, M.W. George, F. Hartl, J.J. Turner, Organometallics 15 (1996) 3374;
(f) D.H. Gibson, H. He, Chem. Commun. (2001) 2082.
[4] P. Christensen, A. Hamnett, A.V.G. Muir, J.A. Tinmey, J. Chem. Soc., Dalton Trans. (1992) 1455.
[5] T. Scheiring, A. Klein, W. Kaim, J. Chem. Soc., Perkin Trans. 2 (1997) 2569.
[6] (a) W. Kaim, S. Kohlmann, Chem. Phys. Lett. 139 (1987) 365;
(b) W. Kaim, S. Kohlmann, Inorg. Chem. 29 (1990) 2909;
(c) H. Hartmann, T. Scheiring, J. Fiedler, W. Kaim, J. Organomet. Chem. 604 (2000) 267.
[7] G.J. Stor, F. Hartl, J.W.M. VanOutersterp, D.J. Stufkens, Organometallics 14 (1995) 1115.
[8] (a) E. Horn, M.R. Snow, Aust. J. Chem. 34 (1981) 737;
(b) D.M. Bruce, A.J. Hewitt, J.H. Holloway, R.D. Peacock, I.L. Wilson, J. Chem. Soc., Dalton Trans. 21 (1976) 2230.
[9] W. Kaim, Coord. Chem. Rev. 219-221 (2001) 463.
[10] S. Frantz, M. Weber, T. Scheiring, J. Fiedler, C. Duboc, W. Kaim, Inorg. Chim. Acta 357 (2004) 2905.
[11] K.P. Darst, C.M. Lukehart, J. Organomet. Chem. 171 (1979) 65.
[12] W. Kaim, S. Kohlmann, J. Jordanov, D. Fenske, Z. Anorg. Allg. Chem. 598–599 (1991) 217.
[13] H. Bock, R. Dienelt, H. Schödel, T.T.H. Van, Struct. Chem. 9 (1998) 279.
[14] M. Krejcik, M. Danek, F. Hartl, J. Electroanal. Chem. 317 (1991) 179.
[15] M. Krejcik, S. Zalis, J. Klima, D. Sykora, W. Matheis, A. Klein, W. Kaim, Inorg. Chem. 32 (1993) 3362.
[16] W. Kaim, Coord. Chem. Rev. 76 (1987) 187.
[17] J.A. Weil, J.R. Bolton, J.E. Wertz, Electron Paramagnetic Resonance, Wiley, New York, 1994.
[18] S. Frantz, H. Hartmann, N. Doslik, M. Wanner, W. Kaim, H.-J. Kümmerer, G. Denninger, A.-L. Barra, C. Duboc-Toia, J. Fiedler, I. Ciofini, C. Urban, M. Kaupp, J. Am. Chem. Soc. 124 (2002) 10563.
[19] C.P. Slichter, Principles of Magnetic Resonance, Springer Series in Solid-State Sciences 1, in: M. Cardona, F. Fulde, K. von Klitzing, H.J. Queisser (Eds.), Springer, Berlin, 1996, p. 507.
[20] (a) D.P. Summers, J.C. Luong, M.S. Wrighton, J. Am. Chem. Soc. 103 (1981) 5238;
(b) W. Kaim, H.E.A. Kramer, C. Vogler, J. Rieker, J. Organomet. Chem. 367 (1989) 107.
[21] W. Kaim, S. Ernst, V. Kasack, J. Am. Chem. Soc. 112 (1990) 173.
[22] G.M. Sheldrick, Programme SHELXS, Göttingen, 1997.
[23] G.M. Sheldrick, Programme SHELXL, Göttingen, 1997.
[24] W. Herrendorf, H. Bärnighausen, Programme HABITUS, Gießen, Karlsruhe, 1993, Gießen, 1996.
[25] CRYSTAL IMPACT Programme DAIMOND, Version 2.1e, Bonn, 2001.